ACS OMEGA

http://pubs.acs.org/journal/acsodf

Article

Air-Processable Perovskite Solar Cells by Hexamine Molecule Phase Stabilization

Nabilah Alias, Akrajas Ali Umar,* Siti Naqiyah Sadikin, Jaenudin Ridwan, Azrul Azlan Hamzah, Marjoni Imamora Ali Umar, Abang Annuar Ehsan, Muhammad Nurdin, and Yiqiang Zhan

Cite This: *ACS Omega* 2023, 8, 18874−18881

Read Online

ACCESS | Metrics & More | Article Recommendations | Supporting Information

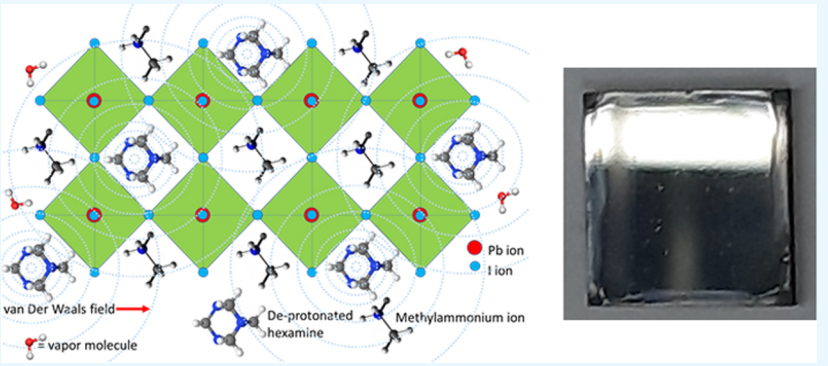

ABSTRACT: Perovskite solar cells have emerged as a potential energy alternative due to their low cost of fabrication and high power conversion efficiency. Unfortunately, their poor ambient stability has critically limited their industrialization and application in real environmental conditions. Here, we show that by introducing hexamine molecules into the perovskite lattice, we can enhance the photoactive phase stability, enabling high-performance and air-processable perovskite solar cells. The unencapsulated and freshly prepared perovskite solar cells produce a power conversion efficiency of 16.83% under a 100 mW cm^{-2} 1.5G solar light simulator and demonstrate high stability properties when being stored for more than 1500 h in humid air with relative humidity ranging from 65 to 90%. We envisage that our findings may revolutionize perovskite solar cell research, pushing the performance and stability to the limit and bringing the perovskite solar cells toward industrialization.

INTRODUCTION

Perovskite solar cells' performance has expanded impressively over the years, and currently, the power conversion efficiency of single-junction solar cells has reached 25.7%. With the advances in preparation,[1] composition, and interfacial engineering,[2,3] the power conversion efficiency of perovskite solar cells is predicted to further ascend, approaching the theoretical limit. At present, techniques for upscaling the perovskite solar cell device have been intensively conducted to meet industrialization criteria.[4] Despite these impressive advances, unfortunately, the reported high-performance perovskite solar cells are still observed under a strictly controlled atmosphere or at most under a relatively dry ambient atmosphere, signifying that the industrialization and commercialization of the device are still obscure. The main reason for this limitation is that the perovskite active material is not stable in a humid environment due to its hygroscopic nature.[5] In many cases, the humidity not only causes extensive roughness to the perovskite film and creates a critical inhomogeneity in the film growth[6] but also degrades the perovskite photoelectrical active phase.[7] Such an effect is even more extensive under the illumination of light or operational temperature[8] as the existence of active ionic migration in the lattice, particularly at the grain boundary, in these circumstances, accelerating the hydration of the perovskite.

There has been an intensive effort in resolving the perovskite's air stability issue over the past several years.[9−13] The introduction of long-chain organic halides or hydrophobic organic spacers[10,14,15] to limit vapor molecules' access to the perovskite's grain boundary has been the most adopted method for this purpose. Long-chain organic halide spacer, for example, normally produces a two-dimensional (2D) perovskite layer on the surface of the perovskite's grain, forming a 2D/three-dimensional (3D) perovskite system. The 2D perovskite layer blocks both the vapor molecules' access and the ionic migration at the perovskite's grain boun-

Received: February 23, 2023
Accepted: April 11, 2023
Published: May 18, 2023

dary,[16−18] but unluckily, it only produces a device that can only be operated in ambient with relative humidity (RH) of around 25%,[18] which is far dry if compared with the real ambient humidity. In addition, because the 2D perovskite has lower carrier mobility and a narrower spectral response window with respect to its 3D counterpart,[19] it significantly reduces the performance of the solar cell. Nonetheless, recent progress in this direction indicates that the oleylamine halide ligand grain surface passivation[16] can realize high-performance and ambient-stable PSC, where it can stand against 85 °C heat and 85% relative humidity. This achievement is certainly phenomenal and promises a big prospect for a real application of perovskite solar cells. Despite this high performance, because their preparation is under a strictly controlled ambient atmosphere with low oxygen and humidity contents, their industrialization prospect could be uncertain. Therefore, the effort to realize air-processable and air-stable perovskite solar cells should be continuously demonstrated.

Here, we report a highly humid-stable methylammonium lead iodide ($MAPbI_3$) perovskite that can stand against a relative humidity of higher than 65% by hexamine molecule phase stabilization. We found that the hexamine molecules' substitution into the perovskite lattice not only stabilizes the lattice dynamics but also preserves its photoactivity properties, realizing exceptionally high-performance and air stability as well as air-processable perovskite solar cells. The perovskite solar cells produce an efficiency of 16.83% under a 100 mW cm^{-2} 1.5G solar light simulator. Meanwhile, the unencapsulated device exhibits excellent stability when being stored in the laboratory ambient with relative humidity ranging from 65 to 90% for 1500 h. The present findings should become a strategic platform for the industrialization of perovskite solar cells.

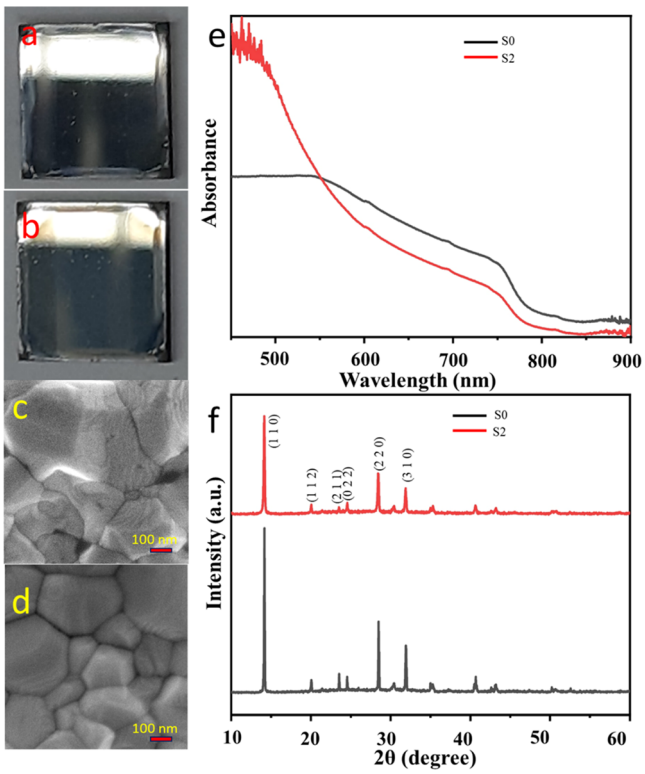

Figure 1. Structural and optical properties of the h-$MAPbI_3$ perovskite. (a, b) Optical images of optimized h-$MAPbI_3$ and pristine $MAPbI_3$. h-$MAPbI_3$ shows a glossy surface. (c, d) Microstructure images of h-$MAPbI_3$ and pristine $MAPbI_3$, respectively. (e) Optical absorbance of the perovskite layer. (f) X-ray diffraction (XRD) patterns for h-$MAPbI_3$ and pristine $MAPbI_3$.

RESULTS

The perovskite solar cells were prepared in the air with an RH of 35−40% (Video S1, Supporting Information). The characteristic of the hexamine-doped $MAPbI_3$ perovskite (h-$MAPbI_3$) and pristine perovskite films produced in this study is smooth, glossy, and mirror-like surfaces (Figure 1a,b). X-ray diffraction pattern analysis (Figure 1f) conveys that the h-$MAPbI_3$ film is a pure cubic phase of perovskite in the absence of the PbI_2 phase. This is highly anticipated as PbI_2 present in the $MAPbI_3$ perovskite triggers the phase transformation of the photoactive cubic $MAPbI_3$ to the inactive delta phase. Our approach also produces pristine $MAPbI_3$ with no PbI_2 phase. Field-emission electron microscopy (FESEM) analysis results discover that, although relatively low crystalline shape, the h-$MAPbI_3$ perovskite grain boundary in this film is diminished, producing a compact film structure. The grain size is up to 300 nm (Figure 1c). Meanwhile, despite the better shape crystallinity and larger gain size of the pristine perovskite film compared with h-$MAPbI_3$, its grain boundary is obvious and prominent (Figure 1d). This might facilitate fast vapor molecule insertion, accelerating phase transformation. The characteristic ultraviolet−visible (UV−vis) absorption spectrum of the film reveals that the optical band gap absorption of the h-$MAPbI_3$ perovskite matches the pristine $MAPbI_3$ perovskite, i.e., in the range of 700 and 800 nm (Figure 1e), rendering that the hexamine substitution maintains the optoelectrical properties of the $MAPbI_3$ perovskite. However, h-$MAPbI_3$ possesses a high absorbance value in the wavelength below 550 nm.

We then fabricated perovskite solar cells with a configuration of ITO/SnO_2/perovskite/P_3HT/Au. The perovskite layer thickness is approximately 390 nm (Figure 2a). Figure 2b shows the typical $J-V$ response of the target perovskite solar cells under the illumination of the solar light simulator (100 mW cm^{-2}). The measurement was carried out in the air with a temperature of ca. ∼25 °C and an RH of higher than 65% (Video S2, Supporting Information). We used a metallic mask (Figure S1, Supporting Information) with a dimension of 4 × 5 mm^2 during the $J-V$ measurement. As the figure reveals, the champion device (i.e., h-$MAPbI_3$) demonstrates an impressively high photovoltaic response with J_{sc}, V_{oc}, and fill factor (FF) as high as 24.40 mA cm^{-2}, 1.11 V, and 62%, respectively. This is equivalent to the power conversion efficiency of 16.83%. Meanwhile, the performance of the control device is far below the target sample, i.e., 3.65%. Low efficiency in the control sample is anticipated and could be related to the phase instability under humid ambient that triggers the perovskite phase transformation, damaging the optoelectrical properties of the perovskite. We have prepared more than 50 h-$MAPbI_3$-based devices (target device) for this condition and found that almost half of the devices have a PCE above 15% (Figure 2f). Figure 1c−f and Table 1 describe the overall performance dynamics of the devices. We then took a device with comparable performance to that of the champion and evaluated the external quantum efficiency properties. We found that the EQE responses of the device (Figure 3a) obey the standard spectral response of the $MAPbI_3$ perovskite and

https://doi.org/10.1021/acsomega.3c01236
ACS Omega 2023, 8, 18874−18881

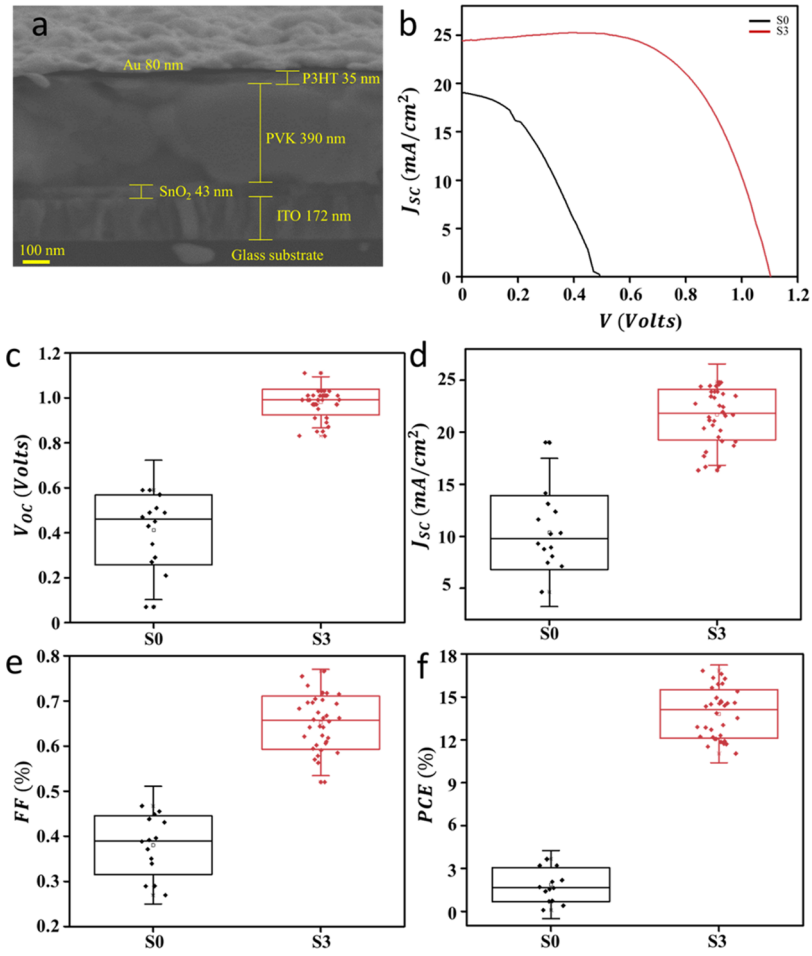

Figure 2. Photovoltaic performance of the perovskite solar cells under 100 mW cm^{-2} 1.5G solar simulator light. (a) Cross-sectional micrograph of the perovskite solar cells. (b) $J-V$ curve of h-$MAPbI_3$ (target device, S3) and pristine (S0) perovskite solar cells under the illumination of 100 mW cm^{-2} solar simulator light. (c–f) Comparison of photovoltaic parameters (V_{oc}, J_{sc}, FF, and PCE) of pristine and champion h-$MAPbI_3$ perovskite solar cells.

Table 1. Photovoltaic Parameters of the Devices[a]

sample	V_{OC} (V) max (avg ± sd)	J_{SC} (mA cm^{-2}) max (avg ± sd)	FF max (avg ± sd)	PCE (%) max (avg ± sd)	R_S (Ω)	R_{ct} (Ω)	R_{rec} (Ω)	trap density, N (cm^3)
S0	0.49 (0.41 ± 0.15)	19.01 (10.36 ± 3.56)	0.39 (0.38 ± 0.07)	3.65 (1.87 ± 1.19)	4.61	62.71	19.27	4.92×10^{22}
S1	1.05 (0.92 ± 0.16)	19.06 (14.82 ± 2.77)	0.67 (0.59 ± 0.09)	13.47 (7.94 ± 2.26)	9.59	7.63	35.58	4.73×10^{22}
S2	1.09 (0.96 ± 0.06)	23.29 (21.12 ± 2.24)	0.65 (0.64 ± 0.07)	16.40 (12.86 ± 1.49)	4.75	6.32	35.74	4.30×10^{22}
S3	1.11 (0.98 ± 0.05)	24.40 (21.70 ± 2.41)	0.62 (0.65 ± 0.06)	16.83 (13.81 ± 1.64)	9.52	16.79	5.768	4.44×10^{22}
S4	1.11 (0.96 ± 0.11)	22.38 (20.06 ± 1.36)	0.61 (0.67 ± 0.07)	15.14 (12.89 ± 1.82)	10.0	27.06	2.249	4.21×10^{22}
S5	1.05 (0.96 ± 0.04)	21.70 (15.43 ± 2.81)	0.66 (0.62 ± 0.03)	15.03 (9.09 ± 1.94)	6.98	26.27	5.296	4.87×10^{22}

[a]S0 = pristine, S1, S2, S3, S4, and S5 are pristine with the addition of 1, 2, 3, 4, and 5 mg mL^{-1} hexamethylenetetramine.

produce a current density comparable to the one obtained in the $J-V$ analysis.

We then stored the unencapsulated device with the initial PCE of 12.5% in the laboratory's ambient atmosphere with a temperature of 25–35 °C and relative humidity of 65–90%, and then gradually evaluated its performance. We found that the target device shows impressively high stability properties when being stored for 1500 h (Figure 3b), which shows a loss in PCE only as low as ca. ∼1%. We expect that the stability could be much longer as the perovskite color is unchanged. However, due to the damage in the metal contact as the result of multiple times measurement processes, device performance could not be measured after that period. For comparison, the control device is immediately damaged if aged for only around 1 h in the ambient atmosphere. The stability properties of the device are also reflected in the maximum power point tracking properties of the device as it retains as high as 94% of the initial efficiency when being operated for 120 s in the ambient atmosphere (Figure 3c). By taking a different device with more or less similar performance, we then evaluated the V_{oc} value of the device as a function of light intensity and discovered that the V_{oc} value decreased as low as only 9.9%, i.e., from 1.01 to 0.91 V, when the light intensity decreased from 100 to 10 mW cm^{-2} (Figure 3d). This implies that the perovskite solar cells can be operated under low light intensity, for example, in indoor applications. The power hysteresis of the device has

https://doi.org/10.1021/acsomega.3c01236
ACS Omega 2023, 8, 18874–18881

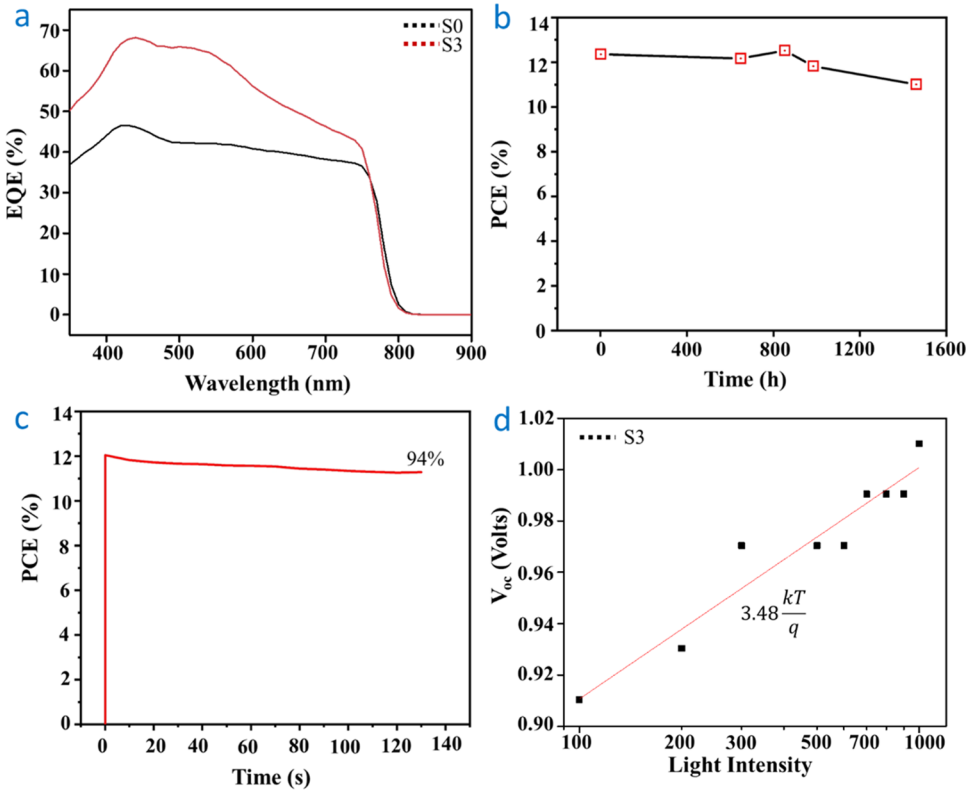

Figure 3. Spectral response and the stability properties of the perovskite solar cells. (a) External quantum efficiency spectra of the champion and the pristine PSC, (b) performance under the aging process in relative humidity of 65−90%, (c) maximum power tracking properties, and (d) double-log plot of the light intensity vs V_{oc}.

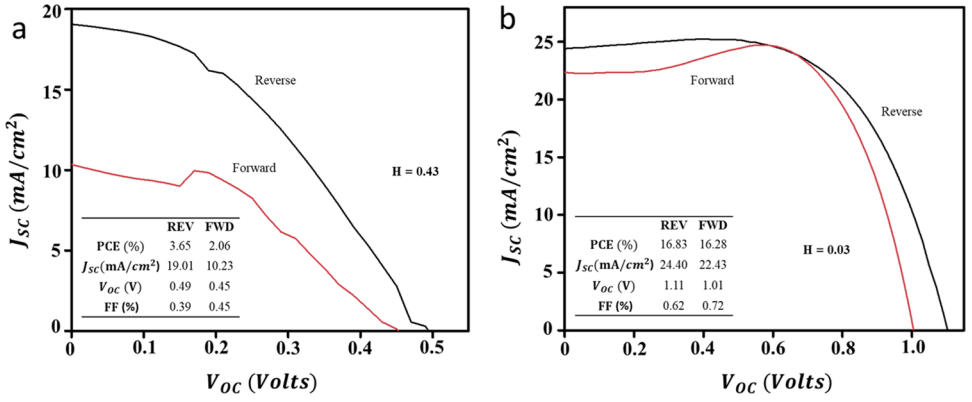

Figure 4. Power hysteresis properties of the device: (a) pristine (S0) and (b) target (S3) devices.

also been evaluated and found that the power hysteresis of the target sample is as low as 3% (Figure 4a). Although the hysteresis value is relatively higher than the recently reported high-performance perovskite solar cells, it is considered low for the perovskite solar cells prepared in the humid ambient. This could be mainly related to several factors, particularly related to the device preparation ambient with high humidity, which causes high-density water molecules present in the vicinity of the perovskite grain surface as well as nonstoichiometric substitution of the hexamine molecules in the lattice, affecting the carrier dynamics in the device under different scan directions. The power hysteresis for the fresh pristine sample is 43% (Figure 4b), which reflects the rapid phase transformation in the perovskite material.

The concentration of hexamine is critical for the phase stability of the perovskite layer. The above-presented results are from the optimized sample that used hexamine with a concentration of 3 mg mL^{-1}. When the hexamine concentration increases or decreases from this condition, the performance reduces (Figure 5). Table 1 and Figure S2 summarize the photovoltaic parameters of the devices and the $J-V$ curves of the champion devices at each condition, respectively. For the sample with a higher hexamine concentration, although the performance was decreased, the obtained perovskite film was more stable when compared to those with a lower concentration as judged from the perovskite color evolution during the aging process (Figure S3, Supporting Information). Lower performance could have resulted from lowered cubic phase $MAPbI_3$ formation at a

https://doi.org/10.1021/acsomega.3c01236
ACS Omega 2023, 8, 18874−18881

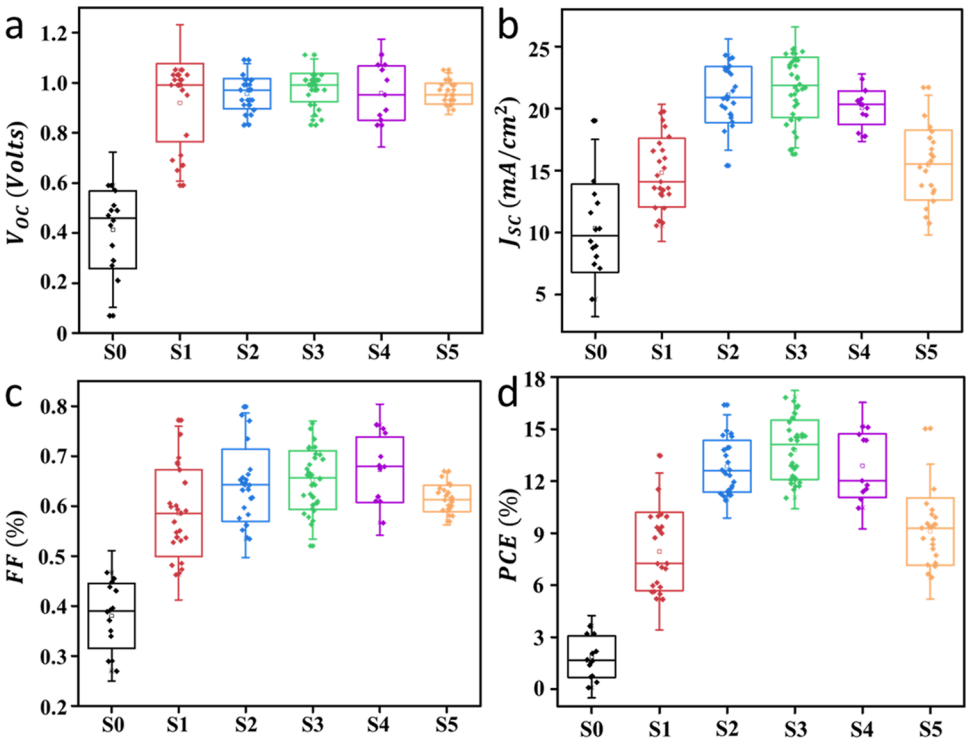

Figure 5. Effect of hexamine concentration on the performance of the solar cell. Statistical distribution of (a) V_{oc}, (b) J_{sc}, (c) FF, and (d) PCE of the perovskite solar cells.

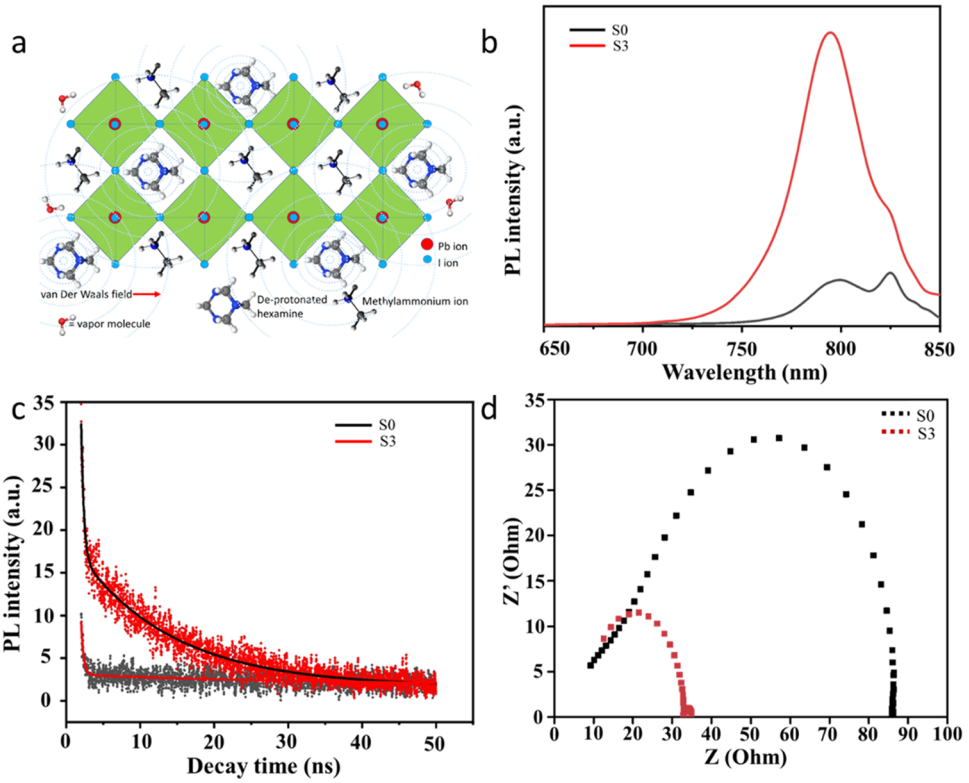

Figure 6. Lattice stability and carrier dynamic properties of the perovskite solar cells devices. (a) van der Waals force effect for lattice stabilization, (b) steady-state, and (c) transient photoluminescences of the perovskite film on a glass substrate. (d) Electrochemical impedance spectra of the device under solar simulator light.

high hexamine concentration as suggested by the XRD analysis results (Figure S4, Supporting Information) that show decrease in the XRD peaks as the hexamine concentration increases. This of course affects its photoelectrical activities, particularly lowering the interfacial charge transfer and increasing the recombination dynamics, thus reducing the

https://doi.org/10.1021/acsomega.3c01236
ACS Omega 2023, 8, 18874−18881

power conversion efficiency (Table 1). Nevertheless, the stability of the perovskite film is relatively lower if compared with the perovskite film in the form of the solar cell device structure. This could be due to the perovskite film directly contacting the atmosphere, which is in contrast to the perovskite layer in the device structure, where it is covered by the P_3HT and gold contact layers so that the direct interaction of vapor to the perovskite layer is limited.

DISCUSSION

The present PSC stability performance is exceptionally high and can stand against relative humidity of higher than 65%. Despite relatively lower performance than those prepared in the controlled ambient, with a PCE that approaches 17%, the present perovskite material system promises industrialization and commercialization prospects. This result signifies that the hexamine molecules have a critical function in stabilizing the phase crystallinity under humid ambient, allowing air-processable perovskite solar cell device. In the present study, considering the preparation process, hexamine molecules should be substituted into the perovskite lattice partly occupying the methylammonium cation site in the entire bulk structure and the surface of the perovskite. Raman analysis results have verified their presence in the perovskite lattice by peaks related to the hexamine molecule vibration mode at 73 and 213 cm^{-1}[20] (Figure S5, Supporting Information), along with Raman characteristics related to Pb−I and methylammonium vibration modes.[21,22] Nevertheless, the exact role of hexamine molecules in the phase stabilization of $MAPbI_3$ perovskite is not yet fully understood at this moment. Nonetheless, the following facts about hexamine properties can be considered as the driving factor for the perovskite stability improvement. (i) Hexamine or hexamethylenetetramine is a diamondoid tetrahedral-cage molecule with an N atom at four vertices of the molecule with a pair of unshared electrons that are linked with each other by the methylene group (Figure S6, Supporting Information). With this chemical structure, hexamine exhibits an active binding property to a large range of atoms or ligands and has been used as an excellent binder or hardener agent, linker, or supporting ligand in coordination chemistry and heavy duty materials.[23,24] This chemical has also been widely used as a directing agent in a growing variety of nanostructures due to its active coordination with the growing crystal plane.[25,26] (ii) In a recent study, hexamine has been reported to form perovskite structures occupying the A site of the lattice in the form of deprotonated hexamine. It has been also discovered that the hexamine molecules in the lattice develop van der Waals force on each other that extends to the entire perovskite lattice,[27] stabilizing the lattice dynamics. Thus, the high air stability of the perovskite's target sample in this study can be related to this phenomenon, where it can harden the lattice and stabilize its dynamics, impedes the ionic migration under a humid atmosphere, and then blocks the phase transformation (Figure 6a). In addition, this molecule was found to facilitate grain enlargement during the aging process as evidenced by the FESEM analysis result (Figure S7). (iii) The absence of the PbI_2 phase in the perovskite film obtained in this study may enhance the stability of the perovskite. Our approach has effectively prepared the perovskite layer with small or no PbI_2 phase both in pristine and h-$MAPbI_3$. As the presence of PbI_2 has been widely understood to drive and accelerate phase transformation in the perovskite, its absence allows highly stable perovskite solar cells under humid conditions.

Photoluminescence spectroscopy analysis results corroborate the last two processes, where the hexamine molecule's substitution into the perovskite lattice improves the PL intensity of the perovskite (Figure 6b). As the PL intensity reflects the quantum yield, a parameter that depends on the crystalline phase quality, the hexamine substitution certainly enhances the photoactive phase stability of the perovskite. The transient PL further confirms these characteristics as the photogenerated carrier lifetime is relatively higher in the target sample (Figure 6c). This certainly suggests that the hexamine molecules enhance both the perovskite photoactive phase crystallinity and stability. This overall process is then manifested into the improvement of the device's carrier dynamics, as verified by the electrochemical impedance spectroscopy results, where the recombination resistance value, as well as interface charge transfer activity in the target device, is significantly higher than in the pristine device (Figure 6d). We carried out a $J-V$ in dark analysis to validate this phenomenon and found that the carrier trap density is impressively low in the target sample (Table 1). This circumstance reveals that the hexamine substitution improves the overall carrier dynamics in the device along with the interface, boosting the power conversion efficiency of the PSC. Despite a relatively high power hysteresis, as discussed earlier, the high efficiency and stability may allow the industrialization of the device.

Considering the nature of the preparation process, which is in high ambient humidity, the typical value of the J_{sc} of the present device is impressively high (i.e., 24.40 mA cm^{-2} for the champion device), challenging the typical best-performed perovskite solar cells that are reported recently. We assume that the following process should be valid, i.e., the existence of highly active interfacial and bulk carrier dynamics in the device. Our present approach produces a perovskite layer with a mirror-like surface. In the typical process, the mirror-like surface reflects that the surface and the bulk structure of the film are highly crystalline, which certainly contains low defect density in the lattice. Photoluminescence analysis verifies this process where the hexamine−perovskite exhibits high PL quantum yield and high carrier lifetime properties. As the mirror-like surface perovskite layer facilitates effective contact with the ETL and HTL layers and low defect density promotes facile carrier transport in the device, their combinative effect will drive massive photocurrent transportation and extraction. Thus, an unusually high photocurrent density is possible. Regarding the power hysteresis issue, as has been mentioned earlier, the hydration of perovskite and the nonstoichiometric substitution of hexamine in the perovskite lattice have caused critical instability in the photogenerated carrier transport in the device. In the pristine sample, the hydration process quickly transformed the perovskite phase, destroying the photoactivity properties of the perovskite. This phenomenon may drive carrier loss in the device as well as at the perovskite−ETL or perovskite−HTL interfaces.[28] Carrier transport instability could have mainly resulted from (i) hexamine molecule-driven carrier trap in the perovskite surface and bulk lattice due to a nonstoichiometric hexamine distribution or molecular segregation. This will cause a loss of photogenerated carrier during the transport, lowering the J_{sc} and V_{oc} values. Controlling the stoichiometric condition of hexamine in the perovskite lattice system and its distribution may alleviate the issue: (ii) surface

https://doi.org/10.1021/acsomega.3c01236
ACS Omega 2023, 8, 18874−18881

roughening by the humidity effect. Surface roughening of the perovskite layer has been among the dominant factors that affect the carrier transport and the interfacial carrier dynamics. Low-magnification FESEM analysis of the perovskite surface likely verified this process, where there is a highly uneven topology as well as a large number of pinholes on the surface of the perovskite layer (Figure S8, Supporting Information). This might occur during the preparation of the perovskite layer under a high humidity level. The perovskite solar cells' performance can be further enhanced when these issues are resolved, for example, via layer postgrowth treatment. We are currently pursuing the study.

As has been earlier mentioned, the nonstoichiometric distribution of hexamine in the perovskite lattice is assumed to be the key origin of the carrier instability in the perovskite solar cell device. Although the exact origin of the non-stoichiometric distribution of hexamine in the perovskite lattice is still not yet understood, we thought that it is due to the limited mixture ability of the hexamine with MAI in the precursor solution. Several approaches, particularly applying the temperature, could be applied to improve the hexamine stoichiometric distribution because the temperature may provide extra kinetic energy to the molecules to achieve equilibrium distribution during the mixing process. Thus, better stoichiometric distribution is expected. Furthermore, the addition of molecular emulsifier addition during the mixing process is also assumed to promote the stoichiometric distribution of hexamine in the perovskite system. As the emulsifier has effectively promoted a better mixing process in a wide range of mixtures, their addition to the perovskite material preparation may improve perovskite crystallinity and optoelectrical and stability properties. Moreover, regarding the stability properties of perovskites in the humid ambient, we assume that it could be further improved if a proper preservation agent is added to the existing formula. As stability in the perovskite is mainly due to the chemical structure transformation due to the hydration (PbI_6^- and MA^+) and ionic migration that occurs in the bulk and the surface causing the surface roughening of the perovskite, the preservative may help retarding such chemical transformation in the perovskite. Combined with already existing stabilization approach, highly stable perovskite solar cells in humid ambient can be obtained.

CONCLUSIONS

We conclude that hexamine molecules stabilize the perovskite lattice, passivating the optoelectrical active phase from transformation under humid ambient. The presence of hexamine has enhanced the phase purity and crystallite size of the perovskite layer, which yields enhanced photoelectrical dynamics in the device. The unencapsulated perovskite solar cells that are stable up to 1500 h in ambient with relative humidity up to 90% can be achieved from this approach. There is indeed a decrease in the efficiency of solar cells after 1500 h. However, it was due to the damage in the metal contact during multiple $J-V$ measurements. Although the power conversion efficiency is relatively lower than the one prepared in controlled ambient, this finding is very remarkable and shows that perovskite solar cells are very resistant to ambient humidity and still exhibit their original properties several days after the manufacture of the device. Having this high stability certainly gives us enough time to make the encapsulation process onto the device, so that a perovskite solar cell system with long stability can be obtained. Also, with these high stability properties, it is possible to fabricate perovskite solar cells in an ambient atmosphere, instead of in a controlled glovebox system, realizing the industrialization prospect.

ASSOCIATED CONTENT

Supporting Information

The Supporting Information is available free of charge at https://pubs.acs.org/doi/10.1021/acsomega.3c01236.

Materials and methods; SnO_2 thin film ETL preparation; perovskite layer preparation; characterizations; metallic mask for $J-V$ analysis of perovskite solar cells; stability properties of the perovskite samples under aging in a relative humidity; Raman spectra of $MAPbI_3$ perovskite in the presence and absence of hexamine; morphology of the perovskite films when being aged in ambient (PDF)

Perovskite solar cell fabrication at ambient conditions (MOV)

Perovskite solar cell characterizations at ambient conditions (MOV)

Solar meter calibration under the sun (MP4)

AUTHOR INFORMATION

Corresponding Author

Akrajas Ali Umar − *Institute of Microengineering and Nanoelectronics, Universiti Kebangsaan Malaysia, UKM, 43600 Bangi, Selangor, Malaysia;* orcid.org/0000-0001-8299-4827; Email: akrajas@ukm.edu.my

Authors

Nabilah Alias − *Institute of Microengineering and Nanoelectronics, Universiti Kebangsaan Malaysia, UKM, 43600 Bangi, Selangor, Malaysia*

Siti Naqiyah Sadikin − *Institute of Microengineering and Nanoelectronics, Universiti Kebangsaan Malaysia, UKM, 43600 Bangi, Selangor, Malaysia*

Jaenudin Ridwan − *Institute of Microengineering and Nanoelectronics, Universiti Kebangsaan Malaysia, UKM, 43600 Bangi, Selangor, Malaysia*

Azrul Azlan Hamzah − *Institute of Microengineering and Nanoelectronics, Universiti Kebangsaan Malaysia, UKM, 43600 Bangi, Selangor, Malaysia*

Marjoni Imamora Ali Umar − *Department of Physics Education, Faculty of Tarbiyah, Universitas Islam Negeri Mahmud Yunus, Batusangkar 27213, Indonesia*

Abang Annuar Ehsan − *Institute of Microengineering and Nanoelectronics, Universiti Kebangsaan Malaysia, UKM, 43600 Bangi, Selangor, Malaysia*

Muhammad Nurdin − *Department of Chemistry, Faculty of Mathematics and Natural Sciences, Universitas Halu Oleo, Kendari 93132, Indonesia*

Yiqiang Zhan − *School of Information Science and Technology, Fudan University, Shanghai 200437, P. R. China;* orcid.org/0000-0001-8391-2555

Complete contact information is available at: https://pubs.acs.org/10.1021/acsomega.3c01236

Author Contributions

N.A. synthesized the perovskite, prepared the device, carried out the analysis, and drafted the manuscript. A.A.U. designed and supervised the project, and finalized the manuscript. S.N.S. along with N.A. synthesized and prepared the device and performed analysis. J.R. along with M.N., and M.I.A.U. carried

https://doi.org/10.1021/acsomega.3c01236
ACS Omega 2023, 8, 18874−18881

out $J-V$, EIS, EQE, and other basic analyses, including FESEM, XRD, and photoluminescence. A.A.H. and A.A.E. provided partial financial support and facilities. Y.Z. provided facilities and result analysis.

Notes

The authors declare no competing financial interest.

■ ACKNOWLEDGMENTS

The authors acknowledge the financial support from the Universiti Kebangsaan Malaysia under DIP-2021-025 and the Ministry of Higher Education under Fundamental Research Grant No. FRGS/1/2019/STG02/UKM/02/3. They also acknowledge the support from the Ministry of Education and Culture of the Republic of Indonesia under the World Class Professor award Grant No. 3252/E4/DT.04.03/2022.

■ REFERENCES

(1) Qiu, F.-Z.; Li, M.-H.; Qi, J.-J.; Jiang, Y.; Hu, J.-S. Engineering inorganic lead halide perovskite deposition toward solar cells with efficiency approaching 20%. *Aggregate* **2021**, *2*, 66−83.

(2) Jeon, N. J.; Noh, J. H.; Yang, W. S.; Kim, Y. C.; Ryu, S.; Seo, J.; Seok, S. I. Compositional engineering of perovskite materials for high-performance solar cells. *Nature* **2015**, *517*, 476−480.

(3) Yoo, J. J.; Seo, G.; Chua, M. R.; Park, T. G.; Lu, Y.; Rotermund, F.; Kim, Y.-K.; Moon, C. S.; Jeon, N. J.; Correa-Baena, J.-P.; et al. Efficient perovskite solar cells via improved carrier management. *Nature* **2021**, *590*, 587−593.

(4) Ding, J.; Han, Q.; Ge, Q.-Q.; Xue, D.-J.; Ma, J.-Y.; Zhao, B.-Y.; Chen, Y.-X.; Liu, J.; Mitzi, D. B.; Hu, J.-S. Fully air-bladed high-efficiency perovskite photovoltaics. *Joule* **2019**, *3*, 402−416.

(5) Song, Z.; Abate, A.; Watthage, S. C.; Liyanage, G. K.; Phillips, A. B.; Steiner, U.; Graetzel, M.; Heben, M. J. Perovskite solar cell stability in humid air: partially reversible phase transitions in the PbI2-CH3NH3I-H2O system. *Adv. Energy Mater.* **2016**, *6*, No. 1600846.

(6) Mesquita, I.; Andrade, L.; Mendes, A. Effect of relative humidity during the preparation of perovskite solar cells: Performance and stability. *Sol. Energy* **2020**, *199*, 474−483.

(7) Yang, J.; Siempelkamp, B. D.; Liu, D.; Kelly, T. L. Investigation of CH3NH3PbI3 degradation rates and mechanisms in controlled humidity environments using in situ techniques. *ACS Nano* **2015**, *9*, 1955−1963.

(8) Zhang, L.; Ju, M.-G.; Liang, W. The effect of moisture on the structures and properties of lead halide perovskites: a first-principles theoretical investigation. *Phys. Chem. Chem. Phys.* **2016**, *18*, 23174−23183.

(9) Wang, X.; Rakstys, K.; Jack, K.; Jin, H.; Lai, J.; Li, H.; Ranasinghe, C. S. K.; Saghaei, J.; Zhang, G.; Burn, P. L. Engineering fluorinated-cation containing inverted perovskite solar cells with an efficiency of> 21% and improved stability towards humidity. *Nat. Commun.* **2021**, *12*, No. 52.

(10) Cho, K. T.; Zhang, Y.; Orlandi, S.; Cavazzini, M.; Zimmermann, I.; Lesch, A.; Tabet, N.; Pozzi, G.; Grancini, G.; Nazeeruddin, M. K. Water-repellent low-dimensional fluorous perovskite as interfacial coating for 20% efficient solar cells. *Nano Lett.* **2018**, *18*, 5467−5474.

(11) Lin, Y.-H.; Sakai, N.; Da, P.; Wu, J.; Sansom, H. C.; Ramadan, A. J.; Mahesh, S.; Liu, J.; Oliver, R. D.; Lim, J.; et al. A piperidinium salt stabilizes efficient metal-halide perovskite solar cells. *Science* **2020**, *369*, 96−102.

(12) Zhao, Y.; Ma, F.; Qu, Z.; Yu, S.; Shen, T.; Deng, H.-X.; Chu, X.; Peng, X.; Yuan, Y.; Zhang, X.; You, J. Inactive (PbI2)2RbCl stabilizes perovskite films for efficient solar cells. *Science* **2022**, *377*, 531−534.

(13) Wu, J.; Liu, S.-C.; Li, Z.; Wang, S.; Xue, D.-J.; Lin, Y.; Hu, J.-S. Strain in perovskite solar cells: origins, impacts and regulation. *Natl. Sci. Rev.* **2021**, *8*, No. nwab047.

(14) Wang, X.; Rakstys, K.; Jack, K.; Jin, H.; Lai, J.; Li, H.; Ranasinghe, C. S. K.; Saghaei, J.; Zhang, G.; Burn, P. L.; Gentle, I. R.; Shaw, P. E. Engineering fluorinated-cation containing inverted perovskite solar cells with an efficiency of >21% and improved stability towards humidity. *Nat. Commun.* **2021**, *12*, No. 52.

(15) Liu, Y.; Akin, S.; Pan, L.; Uchida, R.; Arora, N.; Milić, J. V.; Hinderhofer, A.; Schreiber, F.; Uhl, A. R.; Zakeeruddin, S. M.; Hagfeldt, A.; Dar, M. I.; Grätzel, M. Ultrahydrophobic 3D/2D fluoroarene bilayer-based water-resistant perovskite solar cells with efficiencies exceeding 22%. *Sci. Adv.* **2019**, *5*, No. eaaw2543.

(16) Azmi, R.; Ugur, E.; Seitkhan, A.; Aljamaan, F.; Subbiah, A. S.; Liu, J.; Harrison, G. T.; Nugraha, M. I.; Eswaran, M. K.; Babics, M.; Chen, Y.; Xu, F.; Allen, T. G.; Rehman, Au.; Wang, C.-L.; Anthopoulos, T. D.; Schwingenschlögl, U.; Bastiani, M. D.; Aydin, E.; Wolf, S. D. Damp heat−stable perovskite solar cells with tailored-dimensionality 2D/3D heterojunctions. *Science* **2022**, *376*, 73−77.

(17) Niu, T.; Lu, J.; Jia, X.; Xu, Z.; Tang, M.-C.; Barrit, D.; Yuan, N.; Ding, J.; Zhang, X.; Fan, Y.; Luo, T.; Zhang, Y.; Smilgies, D.-M.; Liu, Z.; Amassian, A.; Jin, S.; Zhao, K.; Liu, S. Interfacial Engineering at the 2D/3D Heterojunction for High-Performance Perovskite Solar Cells. *Nano Lett.* **2019**, *19*, 7181−7190.

(18) Grancini, G.; Roldán-Carmona, C.; Zimmermann, I.; Mosconi, E.; Lee, X.; Martineau, D.; Narbey, S.; Oswald, F.; De Angelis, F.; Graetzel, M.; Nazeeruddin, M. K. One-Year stable perovskite solar cells by 2D/3D interface engineering. *Nat. Commun.* **2017**, *8*, No. 15684.

(19) Katan, C.; Mercier, N.; Even, J. Quantum and Dielectric Confinement Effects in Lower-Dimensional Hybrid Perovskite Semiconductors. *Chem. Rev.* **2019**, *119*, 3140−3192.

(20) Materese, C. K.; Nuevo, M.; Sandford, S. A.; Bera, P. P.; Lee, T. J. The Production and Potential Detection of Hexamethylenetetramine-Methanol in Space. *Astrobiology* **2020**, *20*, 601−616.

(21) Fateev, S. A.; Petrov, A. A.; Khrustalev, V. N.; Dorovatovskii, P. V.; Zubavichus, Y. V.; Goodilin, E. A.; Tarasov, A. B. Solution Processing of Methylammonium Lead Iodide Perovskite from γ-Butyrolactone: Crystallization Mediated by Solvation Equilibrium. *Chem. Mater.* **2018**, *30*, 5237−5244.

(22) Pérez-Osorio, M. A.; Lin, Q.; Phillips, R. T.; Milot, R. L.; Herz, L. M.; Johnston, M. B.; Giustino, F. Raman Spectrum of the Organic−Inorganic Halide Perovskite CH3NH3PbI3 from First Principles and High-Resolution Low-Temperature Raman Measurements. *J. Phys. Chem. C* **2018**, *122*, 21703−21717.

(23) Kirillov, A. M. Hexamethylenetetramine: An old new building block for design of coordination polymers. *Coord. Chem. Rev.* **2011**, *255*, 1603−1622.

(24) Bayol, E.; Kayakırılmaz, K.; Erbil, M. The inhibitive effect of hexamethylenetetramine on the acid corrosion of steel. *Mater. Chem. Phys.* **2007**, *104*, 74−82.

(25) Ali Umar, A.; Oyama, M. High-yield synthesis of tetrahedral-like gold nanotripods using an aqueous binary mixture of cetyltrimethylammonium bromide and hexamethylenetetramine. *Cryst. Growth Des.* **2009**, *9*, 1146−1152.

(26) Vayssieres, L. Growth of arrayed nanorods and nanowires of ZnO from aqueous solutions. *Adv. Mater.* **2003**, *15*, 464−466.

(27) Morita, H.; Tsunashima, R.; Nishihara, S.; Inoue, K.; Omura, Y.; Suzuki, Y.; Kawamata, J.; Hoshino, N.; Akutagawa, T. Ferroelectric Behavior of a Hexamethylenetetramine-Based Molecular Perovskite Structure. *Angew. Chem., Int. Ed.* **2019**, *58*, 9184−9187.

(28) Wang, J. C.; Ren, X. C.; Shi, S. Q.; Leung, C. W.; Chan, P. K. L. Charge accumulation induced S-shape J−V curves in bilayer heterojunction organic solar cells. *Org. Electron.* **2011**, *12*, 880−885.

https://doi.org/10.1021/acsomega.3c01236
ACS Omega 2023, 8, 18874−18881